Mapping the Suramin-Binding Sites of Human Neutrophil Elastase: Investigation by Fluorescence Resonance Energy Transfer and Molecular Modeling†

Yves Mély,‡ Martine Cadène,§ Ingebrigt Sylte,|| and Joseph G. Bieth*,§

Laboratoire d'Enzymologie, INSERM Unité 392, Université Louis Pasteur de Strasbourg, F-67400 Illkirch, France, Laboratoire de Biophysique, CNRS UA 491, F-67400 Illkirch, France, and Institute of Medical Biology, Department of Pharmacology, University of Tromsø, N-9037 Tromsø, Norway

Received May 2, 1997; Revised Manuscript Received July 31, 1997⊗

ABSTRACT: Neutrophil elastase (NE), a mediator of inflammation, binds with high affinity numerous anionic molecules including suramin, a polysulfated naphthylurea, which inhibits it with a K_i of 0.2 μM and a 4:1 suramin:NE stoichiometry and thus constitutes a potential therapeutic agent. In an attempt to locate the suramin molecules on NE, we investigated the NE−suramin interaction using steady-state and time-resolved fluorescence spectroscopy. The time-resolved intensity decay of NE, a protein with three Trp residues, in positions 27, 141, and 237 (chymotrypsin numbering system) was best described by a three-exponential function with lifetimes ranging from 0.22 to 2.28 ns. Comparison of the accessibility of the three lifetime classes to the fluorescence quenchers acrylamide and iodide with the computed solvent accessibility of the three Trp residues in the crystal structure of NE indicates that the main, if not the sole, contribution to the 2.28 ns lifetime class is brought about by the fully buried Trp 141 residue. The addition of suramin to NE induces a sharp decrease in NE fluorescence and a corresponding increase in suramin fluorescence due to an efficient fluorescence resonance energy transfer (FRET) between the Trp residues of NE, acting as donors, and the naphthalene rings of suramin, behaving as acceptors. From the fate of the longest lifetime class in the presence of variable suramin concentrations, we deduce that two suramins are bound at less than 17 Å from Trp 141, whereas the two others are located at least 29 Å from Trp 141. Moreover, neither the binding of suramin to NE nor the FRET process was modified when NE was complexed with a peptide chloromethylketone inhibitor, suggesting that suramin does not directly interfere with the substrate binding site of NE. These data were used as constraints to model the NE−suramin complex.

Neutrophil elastase (NE)[1] is an essential component of the phagocytic machinery of neutrophils, the body's first line of defense against bacterial and fungal attack. NE cleaves extracellular matrix proteins including elastin, interstitial collagen, proteoglycans, fibronectin, and laminin as well as plasma proteins such as antithrombin, fibrinogen and components of the immune system. Uncontrolled release of this enzyme is thought to be involved in chronic inflammation accompanying diseases such as pulmonary emphysema, cystic fibrosis, rheumatoid arthritis, and adult respiratory distress syndrome [for a review see Bieth (1986)].

NE, a 30 kDa glycoprotein belonging to the class of serine proteinases, is composed of 218 amino acid residues with three Trp residues and 19 arginines but no lysines (Sinha et al, 1987). The three-dimensional structure of NE in complex with a synthetic chloromethylketone (MeOSuc-Ala_2-Pro-Ala-CH_2Cl) has been solved by X-ray crystallography (Navia *et al.*, 1989).

NE is known to bind a number of anionic molecules, including heparin, chondroitin sulfate, and unsaturated fatty acids (Redini *et al.*, 1988; Rao *et al.*, 1990; Tyagi & Simon, 1990). Affinities range from 4 nM for a low molecular mass heparin fraction (Cadène *et al.*, 1995) to 16 μM for oleic acid (Tyagi & Simon, 1990). The binding of the polysulfated compound suramin was also demonstrated recently (Cadène *et al.*, 1997). Suramin was found to be a partial tight-binding inhibitor of NE with a K_i of 1.8×10^{-7} M and a 4:1 suramin:NE stoichiometry and may thus be a potential therapeutic agent in acute inflammation. On the other hand, NE increases the intrinsic fluorescence intensity of suramin, and the fluorescence titration of suramin with NE yields a K_d of 2.1×10^{-7} M, thus confirming the enzymatically determined K_i.

The binding of the aforementioned anionic molecules to NE involves positively charged residues of the enzyme, as demonstrated with heparin (Faller *et al.*, 1993), suramin (Cadène *et al.*, 1997), and oleic acid (Tyagi & Simon, 1990). In the last case, the participation of a hydrophobic site on NE in the binding was also evidenced. Though these anions have many features in common in their binding to NE and consequent partial inhibition of the proteinase, it is still unknown whether or not they share the same binding site on NE.

The present paper attempts to locate the suramin molecules on the surface of NE. We have investigated the interaction between these two molecules using both time-resolved fluorescence spectroscopy and FRET. Further information

† This work was supported by grants from the Association française de lutte contre la mucoviscidose.

* Correspondence should be addressed to this author at INSERM U 392, Faculté de Pharmacie, 74 rte du Rhin, F-67400 Illkirch, France. Phone 333.88 67 69 34; Fax 333.88 67 92 42.

‡ Laboratoire de Biophysique.

§ Laboratoire d'Enzymologie, Université Louis Pasteur de Strasbourg.

|| University of Tromsø.

⊗ Abstract published in *Advance ACS Abstracts,* November 15, 1997.

[1] Abbreviations: NE, human neutrophil elastase; MEM, maximum entropy method; IRP, iterative reconvolution procedure; FRET, fluorescence resonance energy transfer; MeOSuc, methoxysuccinyl; *p*NA, *p*-nitroanilide.

S0006-2960(97)01029-5 CCC: $14.00

was also obtained with NE irreversibly inhibited with MeO-Suc-Ala_2-Pro-Val-CH_2Cl. These spectroscopic results, together with previous data on the number of ionic interactions involved in suramin:NE binding (Cadène et al. 1997), were used as constraints to build a structural model of the NE−suramin complex.

EXPERIMENTAL PROCEDURES

NE was isolated from purulent sputum following the procedure of Martodam *et al.* (1979) and active-site-titrated as described by Boudier and Bieth (1992). Suramin (hexasodium *sym*-bis[*m*-aminobenzoyl-*m*-amino-*p*-methylbenzoyl-1-aminonaphthalene-4,6,8-trisulfonate]carbamide) came from Bayer (Germany). The inhibitor MeOSuc-Ala_2-Pro-Val-CH_2-Cl came from Bachem, Bubendorf (Switzerland) and was dissolved in dimethylformamide. All experiments were performed in 50 mM Hepes and 100 mM NaCl, pH 7.4.

Absorption spectra were recorded on a Cary 4 spectrophotometer. An extinction coefficient of 29 800 M^{-1} cm^{-1} at 280 nm was used to calculate the concentration of free NE and MeOSuc-Ala_2-Pro-Val-CH_2Cl-bound NE, whereas an extinction coefficient of 6400 M^{-1} cm^{-1} at 350 nm was used to calculate the concentration of suramin.

Steady-State and Time-Resolved Fluorescence. Fluorescence spectra were acquired at 20 °C with a SLM 48000 spectrofluorometer. Quantum yields were determined by taking L-Trp in water ($\phi = 0.14$) as a reference (Eisinger & Navon, 1969) except for free suramin, which had quinine sulfate in 0.05 M H_2SO_4 as a reference ($\phi = 0.508$; Melhuish, 1961). The NE fluorescence intensities were corrected for inner filter effects due to suramin and scattered light at both excitation and emission wavelengths, with the relation (Pigault & Gérard, 1984)

$$I_p = I_m \frac{(d_p + d_s + d_r/2)\,(1 - 10^{-d_p})}{d_p(1 - 10^{-(d_p + d_s + d_r/2)})} \qquad (1)$$

where I_m is the measured fluorescence of the protein, I_p is the fluorescence intensity of the protein in the absence of inner filter, d_p is the absorbance of the protein, d_s is the absorbance of the suramin and scattered light at the excitation wavelength, and d_r is the absorbance of suramin and scattered light at the emission wavelength.

NE concentrations ranged from 0.48 to 0.6 μM. The NE−MeOSuc-Ala_2-Pro-Val-CH_2Cl complex was prepared by reacting NE with a 15% molar excess of inhibitor during 1 h.

Fluorescence lifetimes were measured with a time-correlated, single-photon counting technique using a pulse-picked frequency-tripled Ti−sapphire laser (Tsunami; Spectra-physics), pumped by a continuous-wave argon laser (Spectra Physics). Temperature was maintained at 20 °C. The excitation and emission wavelengths were set at 295 and 340 nm, respectively. The excitation pulse width was ≤ 2 ps and its repetition rate was 800 kHz. The single-photon pulses were detected with a microchannel plate Hamamatsu R3809U photomultiplier coupled to a Phillips 6954 pulse preamplifier and recorded on a multichannel analyzer (Ortec 7100) calibrated at 26.5 ps/channel. The instrumental response function was recorded with a polished aluminium reflector, and its full width at half-maximum was 40 ps. The decay data were analyzed as a sum of exponentials using the MEM and the Pulse5 software (Livesey & Brochon, 1987). A lifetime domain spanning 150 equally spaced values on a logarithmic scale between 0.05 and 10 ns was routinely used. Alternatively, the decay data were analyzed using IRP based on the estimated covariance matrix (Lami & Piémont, 1992). Since up to 20 decays were accumulated for each sample, confidence intervals of the mean recovered decay parameters were estimated using Hotelling's T^2 statistics. The number of exponentials was progressively increased until the fit (as judged by reduced χ_R^2) did not improve. Noticeably, in almost all cases, the barycenter value (τ_i) and the relative proportion (c_i) of each lifetime class obtained by MEM closely agreed with the respective lifetime (τ_j) and the relative preexponential terms (α_j) obtained from the IRP nonlinear least-squares analysis. The mean fluorescence lifetime is given by $\langle\tau\rangle = \Sigma\, c_i\tau_i$.

The iodide and the acrylamide quenching measurements were carried out using time-resolved fluorescence measurements by adding aliquots of a concentrated solution of potassium iodide (4M) or acrylamide (5M), to NE. The solute quenching data were analyzed by a least squares fit of the lifetimes to the Stern-Volmer equation:

$$\frac{\tau_{i,0}}{\tau_i} = 1 + k_{qi}\tau_{i,0}[Q] \qquad (2)$$

where [Q] is the quencher concentration, k_{qi} is the bimolecular quenching rate constant, and τ_i and $\tau_{i,0}$ are the fluorescence lifetimes, in the presence and absence of the quencher, respectively.

Molecular Modeling Studies. Molecular mechanical energy minimizations and molecular dynamic simulations were performed with the AMBER 4.0 all-atom force field (Weiner et al., 1986). A distance-dependent dielectric function ($\epsilon = r$, where r = interatomic distance) was used to calculate the electrostatic interactions, with a 12 Å cutoff radius for nonbonded interactions. Energy minimizations of NE and NE−ligand complexes were done by 500 steps of steepest descent minimization followed by 3000 cycles of conjugate gradient minimization, while energy minimization of suramin was done until convergence with a 0.02 kcal/mol energy gradient difference between successive steps. Molecular graphics and calculations of water-accessible surface and electrostatic potentials 1.4 Å outside the surface were performed with the MIDAS programs (Ferrin et al. 1988).

The standard all-atom AMBER force field did not contain parameters related to the SO_3-Na groups of suramin. Equilibrium bond lengths and angles, and torsional barrier phase angles for the SO_3-Na groups were obtained from X-ray crystal structures of sodium sulfonate salts (Lefebvre et al., 1992; Kosnic et al., 1992). The bond and angle force constants were set equal to corresponding standard AMBER all-atom force constants, and adjusted until the geometry of the SO_3-Na group observed in the crystal structures was reconstructed by energy minimization of suramin. An initial model of suramin was constructed using the low energy conformation of suramin from a previous molecular modeling study of suramin (Mohan et al., 1991) as a guide. The initial model was energy-optimized without including electrostatic interactions, and the atomic point charges were quantum mechanically calculated with the QUEST 1.0 program (Singh & Kollman, 1984) using an STO-3G basis set. The suramin molecule was then energy-minimized with the electrostatic

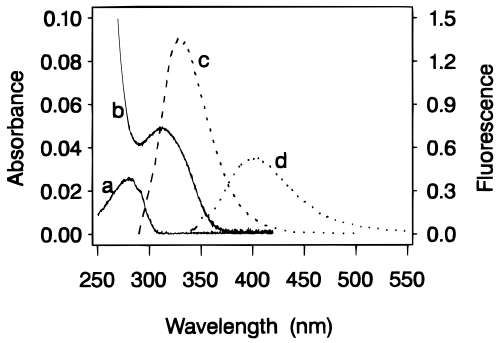

FIGURE 1: Absorbance and fluorescence spectra. Absorbance spectra of NE (a) and suramin (b) and fluorescence emission spectra of NE excited at $\lambda = 295$ nm (c) and of suramin excited at $\lambda = 315$ nm (d) are shown.

interactions included. The structure after the last energy minimization was used as the initial structure in a 50 ps molecular dynamics simulation at 310 K. A time step of 0.001 ps was used, and the nonbonded pair list was updated after every 10 steps. Coordinates were saved at 0.5 ps intervals, and different conformations of suramin observed during the simulation were energy-minimized.

Four suramin molecules were docked at the surface of NE, energy-minimized, and then used as the start structure for a 50 ps molecular dynamic simulation at 310 K. Water molecules were not included in the simulation, and, therefore, a distance-dependent dielectric function ($\epsilon = r$, $r =$ interatomic distance) was used for the electrostatic interactions. The main-chain atoms of NE were kept at fixed positions during the simulation, while the SHAKE option was used to constrain all bonds involving hydrogen atoms. The time step was 0.001 ps, and the nonbonded pair list was updated after every 10 steps. Coordinates were saved at 0.5 ps intervals during the simulation. The coordinates obtained after 50 ps of simulation were energy-minimized and the molecular interaction energies between the suramin molecules and the arginine residues in NE were calculated.

RESULTS AND DISCUSSION

Characterization of the Intrinsic Fluorescence of NE. NE contains three Trp residues in position 12, 127, and 212 of its primary sequence. In the chymotrypsin numbering system, which is frequently used in this class of serine proteinases and will be used throughout the following text, these residues are located at position 27, 141, and 237, respectively. The emission spectrum of NE (Figure 1) is characterized by a maximum emission wavelength of 329 $\pm$ 1 nm, suggesting that the tryptophans, or at least the most emitting ones, are in a rather hydrophobic environment. The low quantum yield ϕ_{295} of NE (Table 1) suggests strong quenching. To further characterize the fluorescence of these tryptophan residues, the time-resolved intensity decay of NE was investigated. Both MEM and IRP analyses suggested the existence of three classes of excited-state lifetimes ranging from 0.24 to 2.26 ns (Table 1). The very good agreement between MEM and IRP results and the narrowness of the three lifetime peaks obtained by MEM strongly suggest that the decay of NE corresponds to discrete exponentials.

In an attempt to determine if one or several lifetimes may be assigned to individual Trp residues, we measured the NE fluorescence quenching by iodide and acrylamide. Iodide is a selective quencher of surface residues, whereas acrylamide quenches both external and embedded Trp residues (Eftink, 1991). The quenching experiments were performed by time-resolved fluorescence (with at least four concentrations of quencher) to directly yield the bimolecular quenching rate constants of each lifetime class (Table 1). In the case of iodide, the bimolecular quenching rate constants, k_{qi}, for the medium- and long-lifetime classes were much lower than the theoretical value of 2.2×10^9 M^{-1} s^{-1} corresponding to the upper limit for a fluorophore fully exposed at the surface of a 30 kDa protein (Johnson & Yguerabide, 1985). To further quantify the accessibility of the three lifetime classes, the fraction of the fluorophores' surface area, f_{MQ}, that is exposed at the surface of the macromolecule was deduced from Figure 2B of Johnson and Yguerabide (1985) using the ratio of k_{qi} to the bimolecular quenching rate constant of free tryptophan ($k_{FQ} = 4.1 \times 10^9$ M^{-1} s^{-1}; Lehrer, 1971). The f_{MQ} values suggest that the Trp residue(s) associated with the short-lifetime class are partly solvent-exposed while the residue(s) associated with the medium- and the long-lifetime classes are fully buried (Table 1). A similar conclusion was reached with acrylamide since the residue(s) associated with the short-lifetime class were again rather accessible, while those associated with the medium- and the long-lifetime classes were poorly accessible and not accessible at all, respectively. This conclusion was further assessed by the comparison with several single Trp-containing proteins since both iodide and acrylamide k_q values for the long-lifetime class were close to those of the fully embedded Trp residue of RNase T1 or *Escherichia coli* asparaginase (Eftink, 1991). The f_{MQ} values were further compared to the relative solvent accessibility of tryptophans in NE as computed by ProExplore (Oxford Molecular, U.K.) using the crystallographic structure of NE in complex with MeOSuc-Ala_2-Pro-Ala-CH_2-Cl (Navia *et al.*, 1989). Tryptophans 27 and 237, close to the protein surface, are 25.2% and 17.5% accessible to solvent, respectively, while tryptophan 141 is totally buried with 0% accessibility to solvent. A similar conclusion was reached when accessibilities were computed from the energy-minimized structure of NE, in the absence of MeOSuc-Ala_2-Pro-Ala-CH_2Cl (see below). Hence, we may reasonably conclude that the main (if not the sole) contribution to the long-lifetime class is brought about by Trp 141, while the main contribution to the short-lifetime class is brought about by Trp 27 and/or Trp 237. The complex behavior of the medium-lifetime class in the absence or presence of suramin (see below) suggests that this class may be assigned to more than one Trp residue.

Steady-State Fluorescence Measurements Of Suramin−NE Complexes. Suramin sharply decreases the intrinsic fluorescence of NE excited at 295 nm in a concentration-dependent manner (Figure 2). As tryptophan emission was gradually quenched, the nonoverlapping area of the suramin spectrum strongly increased, indicating a radiationless energy transfer between the donor (tryptophan) and the acceptor (suramin). This hypothesis is in good keeping with the strong overlap of the emission spectrum of the donor and the absorption spectrum of the acceptor (Figure 1). However, at this stage, we cannot exclude that the tryptophan fluorescence decrease may partly arise from conformational changes induced by the binding of suramin. In the case of suramin, the coexistence of energy transfer and a conformation-associated fluorescence enhancement has been clearly assessed, since a 12-fold quantum yield increase has been

Table 1: Fluorescence Parameters of NE[a]

ϕ^{295}	τ_i	c_i	$\langle\tau\rangle$ (ns)	$\phi^{295}/\langle\tau\rangle$ (s^{-1})	k_{qi}^I (M^{-1} s^{-1})	k_{qi}^I/k_{FQ}	f_{MQ}	k_{qi}^A (M^{-1} s^{-1})
0.085 (±0.002)	0.24 (±0.01)	0.25 (±0.02)	1.41	6.0×10^7	$1.2\ (\pm0.3) \times 10^9$	0.29	0.4	$8.5\ (\pm0.8) \times 10^8$
	1.33 (±0.04)	0.37 (±0.05)			$1.4\ (\pm0.2) \times 10^8$	0.03	≈ 0	$2.4\ (\pm0.2) \times 10^8$
	2.26 (±0.09)	0.38 (±0.04)			$5.4\ (\pm0.5) \times 10^7$	0.01	≈ 0	$<10^8$

[a] Excitation and emission wavelengths were 295 and 340 nm, respectively. The fluorescence lifetimes, τ_i, the relative amplitudes c_i, and the associated standard errors were obtained from MEM analysis, as described under Materials and Methods. The bimolecular quenching rate constants with iodide, k_{qi}^I, and with acrylamide, k_{qi}^A, were determined from time-resolved measurements. The fractional surface area of the fluorophore, f_{MQ}, exposed at the macromolecule surface was calculated as described in the text. The data are expressed as the means ± standard error of the means for ≥ 3 experiments

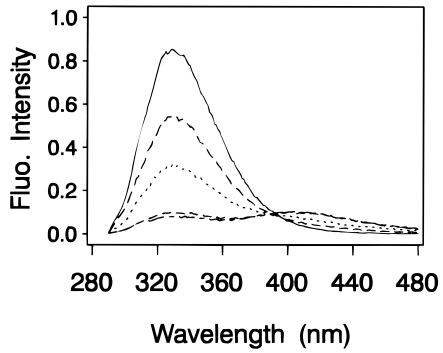

FIGURE 2: Effect of suramin on the fluorescence spectrum of NE. Aliquots of suramin were added to a 0.48 μM NE solution to reach molar ratios of (− −) 1:1, (•••) 2:1, (---) 4:1, and (− - −) 8:1. The spectrum of free NE (—) is also shown. The excitation wavelength was 295 nm. The spectra were corrected for inner filter effects as described under Materials and Methods.

observed at an excitation wavelength of 315 nm where tryptophan does not absorb (data not shown).

To further quantify the transfer process, the transfer efficiency E was calculated by measuring either the sensitized emission of the acceptor or the donor's extinction. In the case of the sensitized emission of suramin, the efficiency, E_A, was obtained through

$$E_A = \frac{A_{A(295)}}{A_{D(295)}}\left(\frac{I_{AD(295)}}{I_{A(295)}} - 1\right) \quad (3)$$

where A_A and A_D are the absorbances of the acceptor and the donor, respectively, whereas I_{AD} and I_A are the fluorescence intensities of the acceptor in the presence and absence of the donor, respectively. I_{AD} and I_A were measured at a 480 nm emission wavelength, where the emission of the donor was negligible (Figure 1). Since both free and bound suramin absorb but only the bound form significantly fluoresces, the absorbance $A_{A(295)}$ was corrected by the fraction of suramin bound to NE calculated from the binding constant. Moreover, for suramin to NE ratios greater than 8, the fluorescence of free suramin was taken into account and substracted. Since there is a conformation-associated emission increase of suramin in the presence of NE in addition to the transfer, $I_{A(295)}$ could not be obtained by a measure of free suramin. Therefore, we straightforwardly deduced the theoretical $I_{A(295)}$ value from the intensity of suramin in the presence of NE at 315 nm, $I_{AD(315)}$, and corrected it for the difference of the absorbances at 295 and 315 nm:

$$I_{A(295)} = \frac{A_{A(295)}}{A_{A(315)}} I_{AD(315)} \quad (4)$$

Table 2: Steady-State FRET Parameters of NE−Suramin Complexes[a]

r	E_D	E_A
0.5	0.17 (±0.02)	0.15 (±0.06)
1	0.33 (±0.02)	0.27 (±0.08)
1.5	0.45 (±0.02)	0.38 (±0.06)
2	0.56 (±0.02)	0.56 (±0.08)
2.5	0.69 (±0.01)	0.66 (±0.08)
3	0.79 (±0.01)	0.79 (±0.1)
4	0.86 (±0.01)	0.90 (±0.1)
5	0.87 (±0.01)	0.95 (±0.1)
6	0.88 (±0.01)	0.97 (±0.1)
8	0.89 (±0.01)	0.96 (±0.1)
16	0.90 (±0.01)	0.96 (±0.1)

[a] The protein concentration was about 0.5 μM. r designates the molar ratio of suramin to NE. The energy transfer efficiencies E_D and E_A, calculated from the donor fluorescence quenching and the acceptor fluorescence enhancement, respectively, were given as the mean (± standard error of the mean) for at least 3 experiments.

Intensities were also corrected for the inner filter effect due to light scattering (Hélène *et al.*, 1971). Efficiencies resulting from the combination of eqs 3 and 4 are reported in Table 2.

The efficiency of transfer, E_D was also calculated from the quenching of NE tryptophans by suramin according to

$$E_D = 1 - \frac{\phi_{DA(295)}}{\phi_{D(295)}} \quad (5)$$

where ϕ_D and ϕ_{DA} are the quantum yields of NE in the absence and presence of suramin, respectively.

The efficiencies obtained from the donor and the acceptor at the various suramin to protein ratios were highly consistent (Table 2): a feature that was, at first glance, somewhat surprising in respect to our fairly complicated system with three donors and four acceptors. However, such a close agreement is favored by several distinctive properties of the system: (i) the prevalence of Trp 141 in the NE fluorescence, since according to the decay parameters of Table 1, at least 61% of the NE fluorescence intensity is due to this residue, (ii) the fluorescence of unbound suramin that is either negligible (at low suramin to NE ratios) or substracted (at high suramin to NE ratios), and (iii) the symmetry of the system since the bound suramin molecules that get small or negligible energy transfer from Trp 141, also get poor energy tranfer from the two other Trp residues (data not shown). Accordingly, we may reasonably suggest that the dramatic decrease in NE fluorescence was entirely due to a nonradiative energy transfer (Schiller, 1975). The existence of FRET in an NE−inhibitor system has previously been reported for the NE−parinaric acid system (Tyagi & Simon, 1991) but with a much lower efficiency.

Table 3: Time-Resolved Fluorescence Parameters of NE−Suramin Complexes[a]

r	τ_i (ns)	c_i	$\langle\tau\rangle$ (ns)	$\phi^{295}/\langle\tau\rangle$ (s^{-1})	$c_{i,c}$	c_0
1	0.23 (±0.03)	0.37 (±0.01)	1.19	4.8×10^7	0.29	0.22
	1.31 (±0.09)	0.30 (±0.05)			0.23	
	2.17 (±0.08)	0.33 (±0.04)			0.26	
2	0.20 (±0.02)	0.52 (±0.01)	0.93	4.0×10^7	0.34	0.35
	1.25 (±0.09)	0.25 (±0.04)			0.16	
	2.25 (±0.09)	0.23 (±0.03)			0.15	
3	0.06 (±0.01)	0.07 (±0.01)	0.54	3.3×10^7	0.04	0.46
	0.17 (±0.01)	0.66 (±0.01)			0.35	
	1.01 (±0.06)	0.15 (±0.01)			0.08	
	2.29 (±0.06)	0.12 (±0.01)			0.07	
4	0.07 (±0.01)	0.10 (±0.02)	0.37	3.2×10^7	0.05	0.48
	0.16 (±0.01)	0.71 (±0.07)			0.37	
	0.78 (±0.01)	0.12 (±0.01)			0.065	
	2.30 (±0.06)	0.07 (±0.01)			0.035	

[a] The experimental conditions, the significance, and the expression of the parameters were as in Tables 1 and 2. The parameters $c_{i,c}$ designate the relative amplitudes recalculated by taking into account the amplitude, c_0, of the undetectably ultrashort lifetime component (<20 ps) as described in the text.

Time-Resolved Fluorescence Measurements of Suramin−NE Complexes. The fluorescence decays of NE in the presence of increasing concentrations of suramin were recorded at 340 nm, an emission wavelength at which the fluorescence of suramin is negligible. Suramin strongly decreases the amplitudes of both medium- and long-lifetime classes (Table 3). In contrast, the amplitude of the short-lifetime class dramatically increases and an even shorter lifetime (60 ps) appears at suramin to protein ratios greater than 3. The long-lifetime value was unaffected by the presence of suramin, while both short and medium lifetimes decreased to some extent. Noticeably, both the narrowness of the various lifetime peaks recovered by MEM in the presence of suramin (data not shown) and the good fits obtained from IRP, assuming discrete exponentials, suggest that the energy transfer process is linked to a narrow distribution of the interchromophore distances (Cheung, 1991). The mean lifetime $\langle\tau\rangle$ gradually decreases in the presence of increasing suramin concentrations, but this decrease is much less pronounced than that of the quantum yields, as assessed by the $\phi_{295}/\langle\tau\rangle$ ratios. As the corresponding fluorescence spectra showed no shift in the maximum emission wavelength, no change in solvent exposure or emitting state was expected (Chen et al, 1991), and hence, the $\phi_{295}/\langle\tau\rangle$ ratio corresponding to the radiative decay rate should not change. Accordingly, the $\phi_{295}/\langle\tau\rangle$ decrease in the presence of suramin may be readily related to a static or quasi-static quenching. This quenching suggests that part of the FRET occurs with an efficiency close to 1 and therefore yields a very short (<20 ps) lifetime that could not be measured by our time-resolved device. The existence of this very short lifetime was further assessed by the data of a ternary complex of suramin bound to NE reacted with an irreversible inhibitor (see below). Consequently, to take into account the amplitude of the negligibly small lifetime, the relative amplitudes $c_{i,c}$ of the various lifetimes in the presence of suramin have been recalculated (Table 3).

Since the long-lifetime class was assigned to Trp 141, the distances of Trp 141 to the four suramin binding sites might be tentatively calculated. From the strong decrease of the relative amplitude of the long-lifetime class in favor of the various short-lifetime classes (< 200 ps) at increasing suramin concentrations (Table 3), we readily infer that the binding of suramin to one or several of its binding sites is

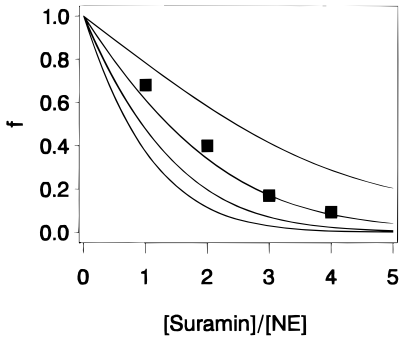

FIGURE 3: Effect of suramin on the concentration of the long-lived fluorescence lifetime of NE. The experimental (■) fractional populations, *f*, of NE with unquenched Trp 141 were calculated from Table 3 as described in the text. Solid lines correspond to the theoretical *f* values, computed from the suramin binding constants. Solid lines were drawn by assuming, from left to right, that zero, one, two or three suramin binding sites are associated with a negligibly small energy transfer efficiency to Trp 141.

associated with a high energy transfer efficiency. By analogy with eq 5, the energy transfer efficiency, E, may be calculated from the lifetime values : $E = 1 - \tau_{DA}/\tau_D$. This calculation suggests that $E > 0.9$ for these suramin binding sites. In contrast, since a nonnegligible fraction of the long-lifetime class remains unquenched even at high suramin to protein ratios, we hypothesized that the binding of suramin to at least one of its binding sites may be associated with a negligibly small energy transfer. To check this hypothesis, we calculated the fractional population, *f*, of NE with unquenched Trp 141 using $f = c_{L,AD}/c_{L,D}$, where $c_{L,AD}$ and $c_{L,D}$ are the relative amplitudes of the long-lifetime class in the presence and absence of suramin, respectively. Assuming that the four suramin binding sites are identical and independent with a 2.1×10^{-7} M equilibrium dissociation constant (Cadène et al. 1997), we computed the theoretical *f* values, assuming that either 0, 1, 2, or 3 binding sites are associated with a negligible E. The data are reported in Figure 3 and clearly suggest that two suramin binding sites are associated with a negligible energy transfer to Trp 141. Since two fluorescence lifetimes can only be resolved if their ratio is greater than 1.4 (Semiarczuk et al., 1990), lifetimes greater than 1.6 ns cannot be distinguished from the 2.26 ns component. As a consequence, binding sites with $E < 0.29$ cannot be detected. Taken together, these data suggest that two suramin binding sites are characterized by an energy transfer efficiency greater

Table 4: Effect of Suramin on the Fluorescence Parameters of NE in Complex with MeO-Suc-Ala_2-Pro-Val-CH_2Cl[a]

r	ϕ_D	E_D	$\tau_{i\,(ns)}$	c_i	$\langle\tau\rangle$ (ns)	$\phi^{295}/\langle\tau\rangle$ (s^{-1})
0	0.084 (±0.002)	0	0.19 (±0.03)	0.24 (±0.02)	1.40	6.0×10^7
			1.09 (±0.04)	0.29 (±0.03)		
			2.22 (±0.02)	0.47 (±0.04)		
2	0.040 (±0.006)	0.52 (±0.03)	0.04 (±0.01)	0.31 (±0.03)	0.66	6.1×10^7
			0.19 (±0.01)	0.36 (±0.02)		
			1.08 (±0.02)	0.14 (±0.01)		
			2.23 (±0.02)	0.19 (±0.01)		
4	0.013 (±0.002)	0.85 (±0.03)	0.05 (±0.01)	0.49 (±0.05)	0.22	5.9×10^7
			0.18 (±0.01)	0.41 (±0.05)		
			0.68 (±0.01)	0.06 (±0.01)		
			2.10 (±0.02)	0.04 (±0.01)		

[a] Experimental conditions, significance and expression of the parameters were as in Table 2 and 3.

than 0.9, while the two others have an energy transfer efficiency lower than 0.29.

To determine the distances between Trp 141 and the four bound suramin molecules, the Förster critical distance, R_0, was further needed and was calculated using

$$R_0^{\,6} = (8.79 \times 10^{-25})\kappa^2 n^{-4}\,\phi_D\,J_{AD} \qquad (6)$$

where the overlap integral (computed from the spectral overlap in Figure 1) $J_{AD} = 9.85 \times 10^{-15}$ M^{-1} cm^6, the refractive index, $n = 1.335$, and the orientational factor, $\kappa^2 = {}^2/_3$, assuming that the donor and the acceptor undergo a complete dynamic isotropic orientational averaging. The quantum yield, ϕ_D, associated with the long-lifetime class was calculated from: $\phi_D = \tau_L\phi^{295}/\langle\tau\rangle$, where ϕ^{295} and $\langle\tau\rangle$ are the quantum yield and the mean fluorescence lifetime of NE, respectively, while $\tau_L = 2.26$ ns. A R_0 value of 25 Å was found and used to calculate the interchromophore distance R:

$$R = R_0[(1/E) - 1]^{1/6} \qquad (7)$$

From eq 7, we infer that two suramin molecules are located at less than 17 Å from Trp 141, while the two others are distant by at least 29 Å from Trp 141. Since the suramin chromophores involved in FRET are undoubtely the two naphthalene groups, these distance limits correspond to the distance between the indole ring of Trp 141 and the closest naphthalene ring of the suramin molecules. The above distances may be slightly different if the orientational factor, κ^2, between the donor and the acceptor molecules is either very low (in the case of perpendicular orientation) or very high (in the case of collinear orientation).

Binding of Suramin to the NE−MeOSuc-Ala_2-Pro-Val-CH_2Cl Complex. In order to get further structural information on the suramin binding site(s), NE was reacted with the irreversible inhibitor MeOSuc-Ala_2-Pro-Val-CH_2Cl, which forms a stoichiometric covalent complex by alkylating the active-site histidine in NE (Navia et al., 1989). Interestingly, the binding of this inhibitor to NE did not significantly change the emission spectrum and the quantum yield of the enzyme (Table 4). While the mean fluorescence lifetime was unchanged, both the medium-lived component and its relative amplitude were somewhat decreased as compared with free NE. Since the spectroscopic properties of Trp residues are extremely sensitive to conformational changes in protein even if the latter are very small, we may safely conclude that the presence of chloromethylketone has at best a marginal effect on the environment of tryptophan residues of NE. This is consistent with the three-dimensional structure of NE in complex with MeOSuc-Ala_2-Pro-Ala-CH_2-Cl (Navia et al., 1989) which shows that the three Trp residues are remote from the bound chloromethylketone, Trp 141 being distant by about 13.4 Å from the covalent enzyme−inhibitor bond. To confirm the lack of influence of the inhibitor on the environment of the Trp residues, we have compared the X-ray crystal structure of the NE−inhibitor complex (Navia et al, 1989) with that of the energy-minimized structure of free NE as obtained by removing the inhibitor from the above crystal structure. This showed that binding of the inhibitor does not modify the environment of the Trp residues and leads to only limited conformational changes in NE, thus entirely confirming the spectroscopic data. We, therefore, conclude that the NE−chloromethylketone complex is a fairly good model of the three-dimensional structure of NE.

Fluorescence titration (Cadène et al. 1997) indicates that the chloromethylketone complex binds suramin with a 1:4 stoichiometry and a K_D of 2.3×10^{-7} M, a value very close to that found for free NE (data not shown). The variations of the lifetimes and the quantum yields in the presence of suramin are similar to those observed with noninhibited NE (Table 4). However, in contrast to noninhibited NE, the ultrashort lifetime (40 ps) could be directly measured for the ternary NE−chloromethylketone−suramin complexes so that the $\phi^{295}/\langle\tau\rangle$ values were constant. The fractional populations of inhibited NE with unquenched Trp 141 were thus directly calculated from the relative amplitudes and were indistinguishable from those of the noninhibited NE (Figure 3). Taken together, our data strongly suggest that the presence of the chloromethylketone inhibitor in the NE active site does not perturb the FRET between Trp 141 and the four bound suramins. In turn, this suggests that suramin does not bind to subsites S_4-S_1 of the enzyme's substrate-binding site and that the suramin-promoted inhibition of enzyme activity (Cadène et al., 1997) is probably due to an indirect effect of the ligand on the enzyme's active site.

Molecular Modeling of NE Complexed to Four Suramin Molecules. In a first step, using the low-energy conformation of suramin from a previous molecular modeling study (Mohan et al., 1991), we performed an energy minimization followed by a 50 ps molecular dynamic simulation in order to find the low-energy conformation of suramin. This analysis yielded five different low-energy conformations of suramin within an energy range of 10.2 kcal/mol, suggesting that suramin is a flexible molecule. A helix-like structure was, however, present in all these conformations. Structural

Table 5: Molecular Interaction Energies and Distances Recovered from Molecular Dynamics Simulation of the NE−Suramin Complex[a]

suramin molecule			
number	naphthalene group[b]	E_{int}[c] (kcal/mol)	D_{Trp141}[d] (Å)
1	A	Arg 36, 86.1; Arg 76, 78.7	12.5
	B	Arg 147, 76.9; Arg 149, 75.2	17.9
2	A	Arg 20, 37.8; Arg 186, 67.3; Arg 187, 65.0	13.1
	B	Arg 21, 73.6; Arg 23, 60.0; Arg 75, 44.6	20.8
3	A	Arg 177, 58.8; Arg 178, 51.0; Arg 217A, 46.0	28.6
	B	Arg 128, 70.9; Arg 129, 81.2	30.9
4	A	Arg 63, 73.8; Arg 87, 50.7	27.7
	B	Arg 178, 66.4	33.9

[a] Both the molecular interaction energies, E_{int}, between the arginine side chains of NE and the naphthalene rings of suramin and the distances, D_{Trp141}, between Trp 141 and the naphthalene rings were recovered after 50 ps of molecular dynamics simulation and energy minimization, as described in the text. [b] Suramin is a symmetrical molecule with two identical naphthalene groups (Nakajima et al., 1991). These groups have been arbitrarily labeled A and B, according to their proximity with Trp 141, A being, in each case, the closest to Trp 141. [c] E_{int} are reported in absolute values and only those larger than 20 kcal/mol are given. [d] D_{Trp141} was measured between the centers of the indole and the naphthalene rings.

flexibility of ligands causes difficulties when protein−ligand interactions are studied by molecular modeling techniques. In order to partly solve this problem and avoid unfavorable nonbonded interactions, a molecular dynamics simulation was performed to refine the interactions between the four suramin molecules and NE. Water molecules were not included in the simulation, the main-chain atoms of NE were kept at fixed positions, and the simulation was not performed for more than 50 ps, so that the simulation should not be considered as a study of time-dependent structural changes of the NE−suramin complex. Four suramin molecules were docked at the surface of the energy-minimized structure of NE, the docking criteria being the complementarity in electrostatic potentials between suramin and NE and the distance constraints inferred from fluorescence data in the absence and presence of suramin. Conformations different from the observed lowest energy conformations of suramin were also docked at the surface of NE, but these dockings did not change the conclusions concerning the binding of suramin to NE.

Several positions of suramin relative to NE were considered. Among them, the suramin−NE complex shown in Figure 4 was found to be most in agreement with the docking criteria. The molecular interaction energies between the arginine side chains of NE and the naphthalene rings of suramin as well as the distances between Trp 141 and each naphthalene ring are given in Table 5. In good keeping with the FRET data, the naphthalene rings of suramin that are the closest to Trp 141 are located 12.5, 13.1, 28.6, and 27.7 Å from the indole ring of this residue (see also Table 5). The two latter distances are slightly lower than expected. This is due to the fact that both naphthalene groups are in a perpendicular orientation relative to the indole ring of Trp 141, which markedly decreases the FRET. On an overall basis, however, the model is in agreement with the FRET data, which demonstrates that two suramin molecules are located at less than 17 Å from Trp 141 while the two other suramins are distant by at least 29 Å from this residue. We also checked whether the model is consistent with the interaction of suramin with the Arg residues of NE. In good agreement with the observation that an average of four ionic interactions takes place per molecule of bound suramin (Cadène et al., 1997), we found that suramins 1, 2, 3, and 4 interact strongly with four, six, five, and three Arg residues, respectively.

Conclusion. NE has been shown to bind numerous anionic ligands; we report here the first structural model of its complex with such a compound. This model was built using the FRET data as constraints for molecular modeling. FRET data have previously been used in an attempt to locate the binding site of the hydrophobic inhibitor parinaric acid to NE (Tyagi & Simon, 1991). However, in the latter case, the study was performed by steady-state fluorescence and only a mean distance between the three Trp residues of NE and the inhibitor could be inferred. Using time-resolved fluorescence spectroscopy, we unambigously assessed that the long-lifetime class was mainly contributed by Trp 141 and thus we directly determined the distance between this Trp and the four bound suramins. A second feature that significantly simplified the analysis of this apparently sophisticated system was that the suramin molecules bound to NE had an all-or-none behavior as far as FRET is concerned.

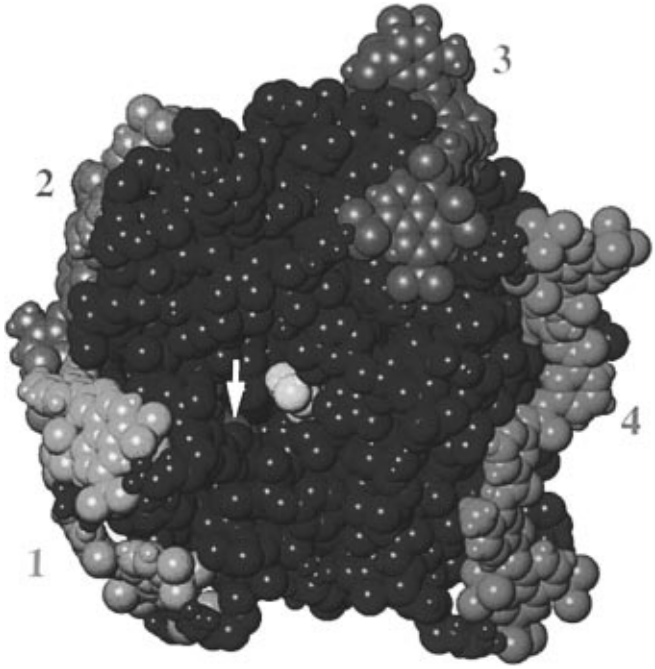

FIGURE 4: Space-filling model of the NE−suramin complex. The numbering of the four suramin molecules is as in Table 5. The centrally located yellow residue is Ser 195 of the catalytic site of NE. The green residue shown by an arrow is Trp 141. To make this buried residue visible, Cys 191, Phe 192, and Gly 193 have been deleted.

Of course, a further and definitive assessment of this model requires X-ray crystallography of the complex. Nonetheless, this model constitutes a good start to determine whether other

anionic molecules such as heparin or polynucleotides that also inhibit NE, and are thus potential therapeutic agents, share common binding sites with suramin. This should easily be performed by competition experiments, using FRET techniques.

ACKNOWLEDGMENT

We thank Dr. D. Gérard for helpful suggestions and for carefully reading the manuscript.

REFERENCES

Bieth, J. G. (1986) in *Biology of the Extracellular Matrix* (Mecham, R. P., Ed.) Vol. 1, pp 217−320, Academic Press, Inc., New York.
Boudier, C., & Bieth, J. G. (1992) *J. Biol. Chem. 267*, 4370−4375.
Cadène, M., Boudier, C., De Marcillac, G., & Bieth, J. G. (1995) *J. Biol. Chem. 270*, 13204−13209.
Cadène, M., Duranton, J., North, A., Si-Tahar, M., Chignard, M., & Bieth, J. G. (1997) *J. Biol. Chem. 272*, 9950−9955.
Chen, R. F., Knuston, J. R., Ziffer, H., & Porter, D. (1991) *Biochemistry 30*, 5184−5195.
Cheung, H. C. (1991) in *Topics in Fluorescence Spectroscopy* (Lakowicz, J. R., Ed.) Vol. 2, pp 141−176, Plenum Press, New York.
Eftink, M. R. (1991) in *Topics in Fluorescence Spectroscopy* (Lakowicz, J. R., Ed.) Vol. 2, pp 53−120, Plenum Press, New York.
Eisinger, J., & Navon, G. (1969) *J. Chem. Phys.* 50, 2069−2077.
Ferrin, T. E., Huang, C. C., Jarvis, L. E., & Langridge, R. (1988) *J. Mol. Graphics 6*, 13−27.
Frigerio, F., Coda, A., Pugliese, L., Lionetti, C., Menegatti, E., Amiconi, G., Schnebli, H. P., Ascenzi, P., & Bolognesi, M. (1992) *J. Mol. Biol. 225*, 107−123.
Hélène, C., Brun, F., & Yaniv, M. (1971) *J. Mol. Biol. 58*, 349−365.
Hyberts, S. G., Goldberg, M. S., Havel, T. F., & Wagner, G. (1992) *Protein Sci. 1*, 736−751.
Johnson, D. A., & Yguerabide, J. (1985) *Biophys. J. 48*, 949−955.
Kosnic, E. J., McClymont, E. L., Hodder, R. A., & Squattrito, P. J. (1992) *Inorg. Chim. Acta 201*, 143−151.
Lami, H., & Piemont, E. (1992) *Chem. Phys. 163*, 149−159.
Lefebvre, J., Miniewicz, A., & Kowal, R. (1992) *Acta Crystallogr. C48*, 612−615.
Lehrer, S. S. (1971) *Biochemistry 10*, 3254−3263
Livesey, A. K., & Brochon, J. C. (1987) *Biophys. J. 52*, 693−706.
Martodam, R. P., Twumassi, D. Y., & Liener, I. E. (1979) *Prep. Biochem. 9*, 15−31.
Melhuish, W. H. (1961) *J. Phys. Chem. 65*, 229−241.
Mohan, P., Hopfinger, A. J., & Baba, M. (1991) *Antiviral Chem. Chemother. 2*, 215−222.
Nakajima, M., De Chavigny, A., Johnson, C. E., Hamada, J., Stein, C. A., & Nicolson, G. L. (1991) *J. Biol. Chem. 266*, 9661−9666.
Navia, M. A., McKeever, B. M., Springer, J. P., Lin, T. Y., Williams, H. R., Fluder, E. M., Dorn, C. P., & Hoogsteen, K. (1989) *Proc. Natl. Acad. Sci. U.S.A. 86*, 7−11.
Pigault, C., & Gérard, D. (1984) *Photochem. Photobiol. 40*, 291−296.
Rao, N. V., Kennedy, T. P., Rao, G., Ky, N., & Hoidal, J. R. (1990) *Am. Rev. Respir. Dis. 142*, 407−412.
Redini, F., Tixier, J. M., Petitou, M., Choay, J., Robert, L., & Hornebeck, W. (1988) *Biochem. J. 252*, 515−519.
Schiller, P. W. (1975) in *Biochemical Fluorescence Concepts* (Chen, R. F., & Edelhoch, H., Eds.) Vol. 1, pp 285−303, Marcel Dekker, Inc., New York.
Semiarczuk, A., Wagner, B. D., & Ware, W. R. (1990) *J. Phys. Chem. 94*, 1661−1666.
Singh, U. C., & Kollman, P. A. (1984) *J. Comput. Chem. 5*, 129−145.
Sinha, S., Watorek, W., Karr, S., Giles, J., Bode, W., & Travis, J. (1987) *Proc. Natl. Acad. Sci. U.S.A. 84*, 2228−2232.
Tyagi, S. C., & Simon, R. S. (1990) *Biochemistry 29*, 9970−9977.
Tyagi, S. C., & Simon, R. S. (1991) *J. Biol. Chem. 266*, 15185−15191.
Weiner, S. J., Kollman, P. A., Nquyen, D. T., & Case, D. A. (1986) *J. Comput. Chem. 7*, 230−252.

BI971029R